Supporting Information

All-direction energy harvester based on nano/micro fibers as flexible and stretchable sensors for human motion detection

Yiin-Kuen Fuh[1], Po-Chou Chen[1], Hsi-Chun Ho[1], Zih-Ming Huang[1], Shang-Cian Li[1]

[1]*Department of Mechanical Engineering, National Central University, No.300, Jhongda Rd., Jhongli District, Taoyuan City 32001, Taiwan (R.O.C.)*

Corresponding author: Dr. Yiin-Kuen Fuh

Mailing Address: Department of Mechanical Engineering, National Central University, No.300, Jhongda Rd., Jhongli City, Taoyuan County 32001, Taiwan (R.O.C.)

Telephones: +886- 03-4267305 (office)

Fax: +886- 03-4254501

E-mail: michaelfuh@gmail.com/stuvwxyz0618@gmail.com

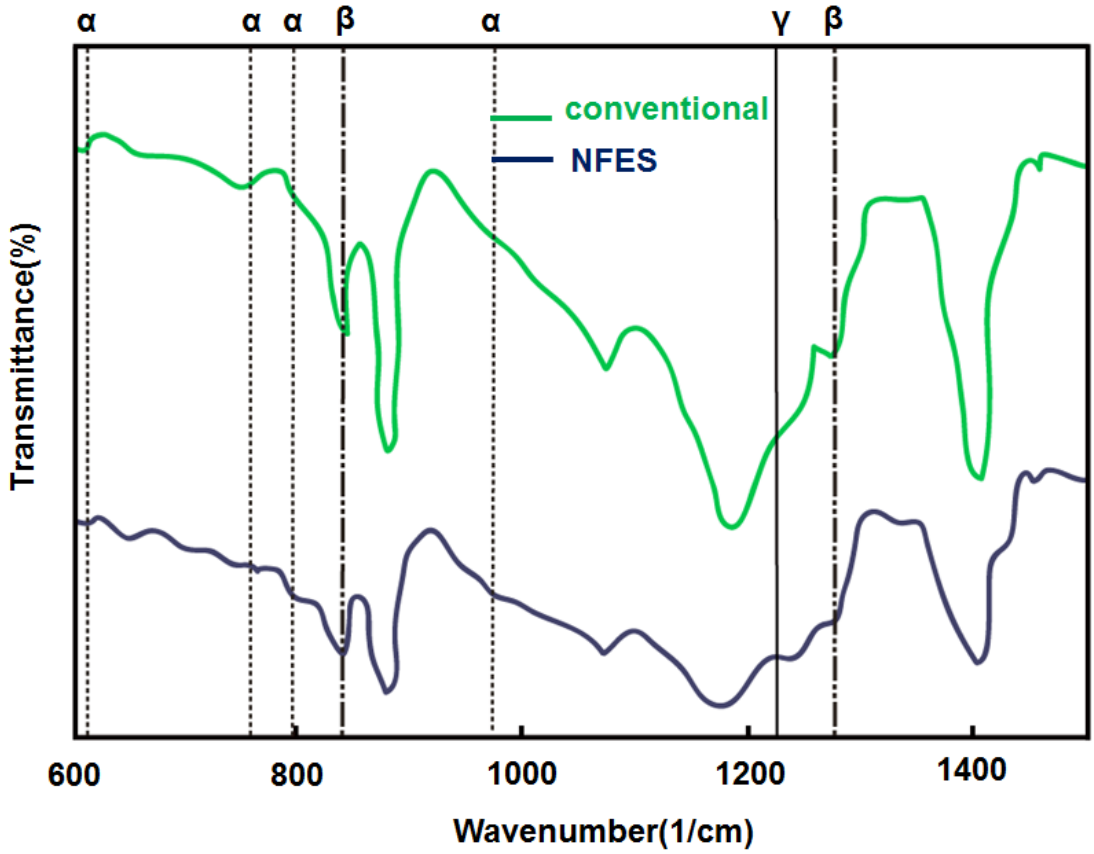

Fig.S1 FTIR spectra of NFES with the needle-to-collector distance is 1mm/applied voltages 1kV and conventional electrospinning with 10kV15cm from a PVDF in DMF/acetone solution.

Fig.S1 shows FTIR spectra of both NFES and conventional electrospinning samples for the purpose of investigating the bonding structure of various electrospun PVDF nanofibers, It is observed that FTIR spectra of NFES samples exhibit the α-phase related bands at 614, 760, 795 and 975 cm^{-1} and the β-phase related bands at 840 and 1278 cm^{-1}, respectively. In comparison, the conventional electrospinning fibers share the similar characteristics in α-, β- and γ-phase related bands. However, the NFES fibrous membranes exhibit weaker and broad diffraction peaks, which may be attributed to the small size of the crystallites. [W. A. Yee, M. Kotaki, Y. Liu, and X. Lu, Polymer, 48, 512–521, 2007.]

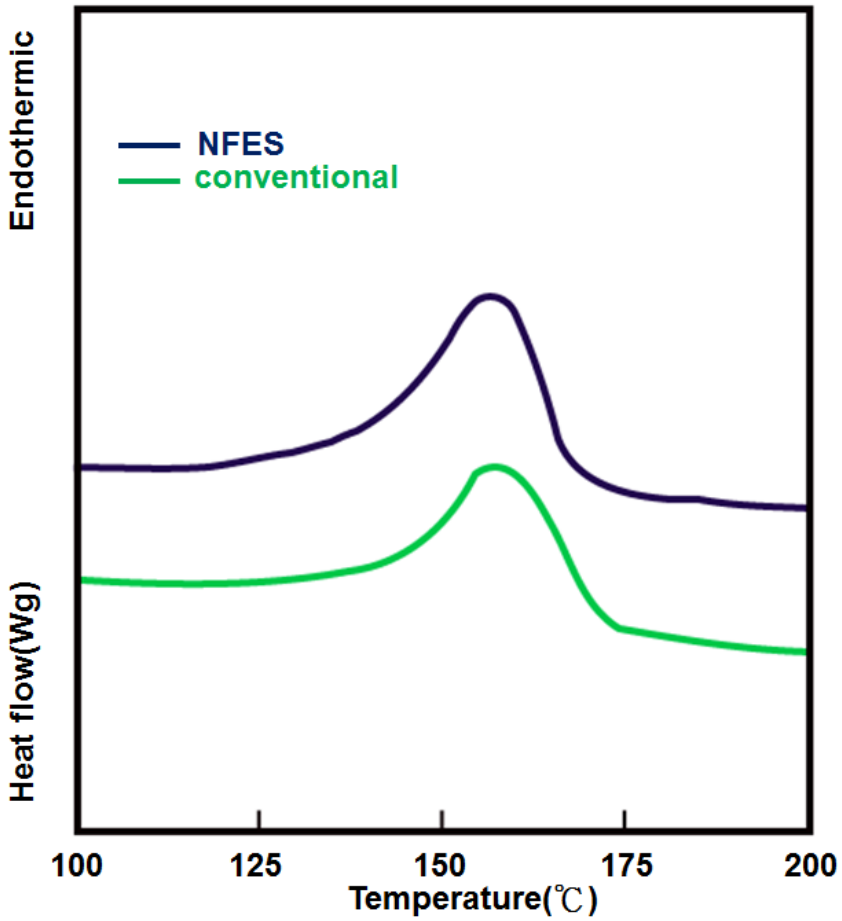

Fig.S2 Modulated DSC thermograms of NFES with applied voltages 1kV and conventional eletrospinning applied voltage 10kV respectively.

DSC measurements are carried out for clarifying the possible modifications in crystal structure. Fig.S2 shows the DSC scans of the samples. It is observed that all samples have almost similar endothermic peaks extending from 150°C to 175 °C. This result is analogous to the report of Gao et al. [K. Gao, X. Hu, C. Dai, T. Yi, Mater. Sci. Eng. B, 131, 100–105, 2006.], they measured PVDF fibers with diameters from 514nm to 884nm and showed similar endothermic peaks from 155°C to 173 °C. Although manufacturing processes of the fibers are not identical and fibers diameters are different, however, it is experimentally observed that the both NFES and conventional electrospinning samples share similar characteristics in melting and endothermic values.

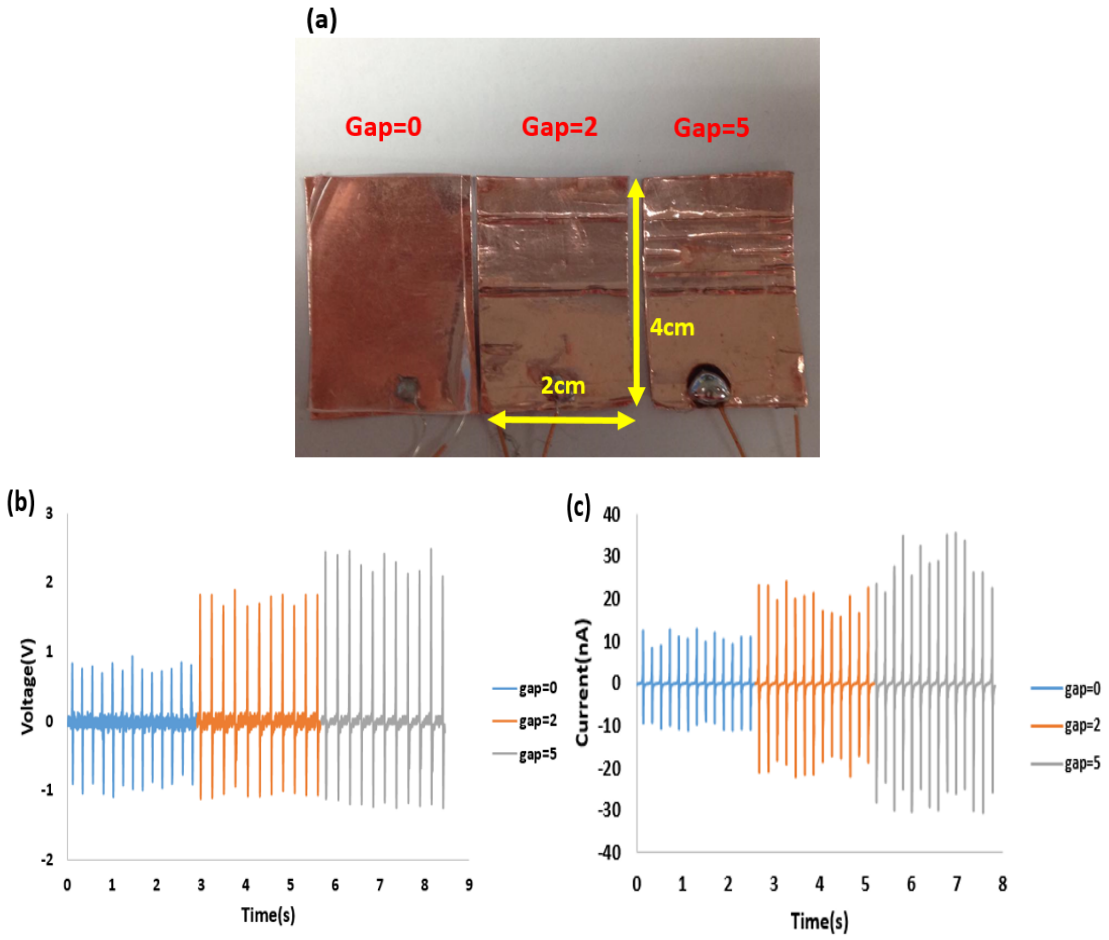

Fig.S3 Electrode gap effect with (a) zero gap, two gaps, and five gaps.

In order to prove that the PG could harvest not only continuous fibers but also integrations of multiple discontinuous or separated NMFs from each respective electrode, we tested three samples with three different layouts, showing the same copper substrate (2cm width by 4cm length) covered with no gap, 2 and 5 gaps respectively. Each gap has a dimension of 2cm×0.015cm×0.015cm. The design reported here, NMFs settle between two random electrodes on a flexible substrate. When stretched and released the NMFs of PG at 4Hz and strain of 0.5%, the integration of NMFs with harvested energy is increased from 0.9V/10nA to 2.1V/25nA for the same copper substrate of zero gap and five gaps respectively. This result showed that the output performance in both voltage (b) and current (c) would increase incrementally as the number of gaps increased at 4Hz and strain 0.5% flapping motion.

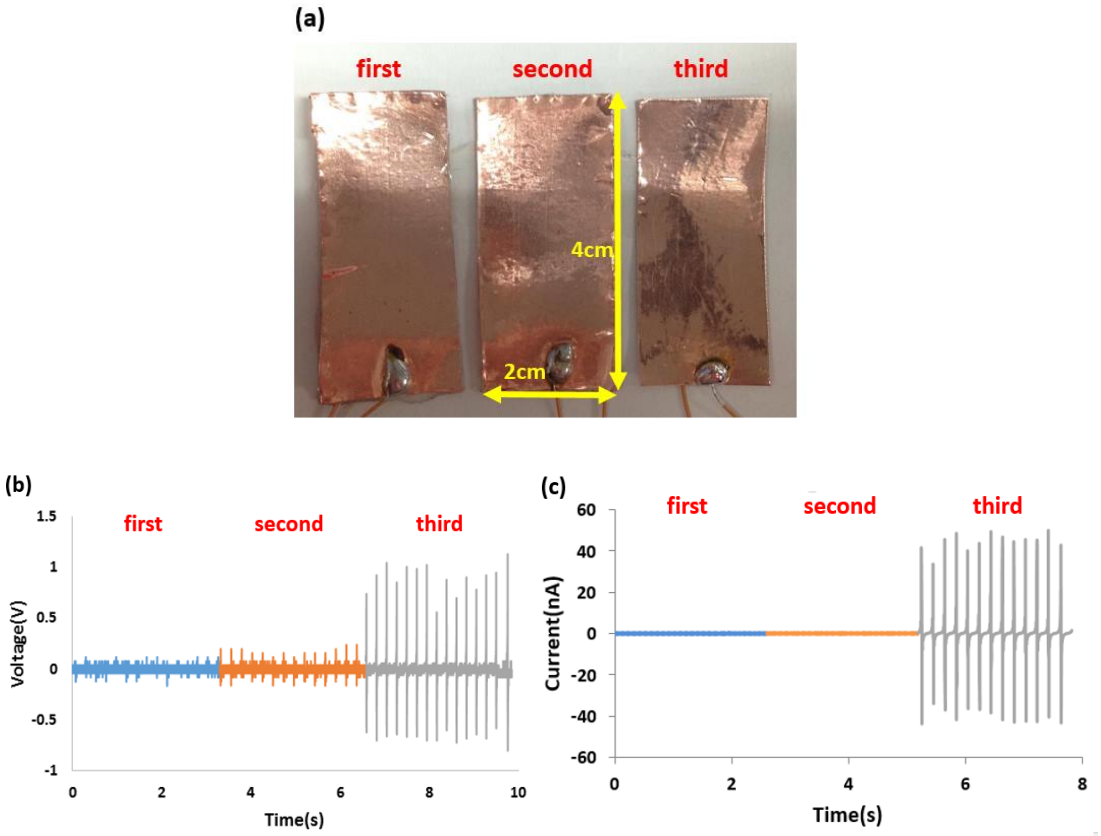

Fig.S4 The design control experiment excluded the triboelectric effect. We tested three kinds of samples (a) the first sample was the substrate without fibers, the second sample was the substrate with PVDF conventional electrospinning NMFs, and the third sample was the substrate with PVDF NFES NMFs. The output voltage (b) and current (c) showed only noise signals when flapped the substrate without PVDF NFES NMFs at 4Hz and strain 0.5%.

To verify that the electrical outputs were generated from piezoelectric properties of PVDF NMFs and exclude the triboelectric effect, we performed the same experiments but change three kinds of samples. The output voltage and current (Fig.S4 (b) (c)) showed that only the noise signals were observed in first sample (no PVDF NMFs). The second sample (conventional electrospinning PVDF NMFs) showed very small outputs were generated due to the random polarity of electrospinning PVDF NMFs would strongly abate the output performance of PG. Last, the third sample (PVDF NFES) showed obviously voltage and current than the first and second samples. The data precluded the possibility of triboelectric as the cause of the observed electric outputs for the PVDF NFES.

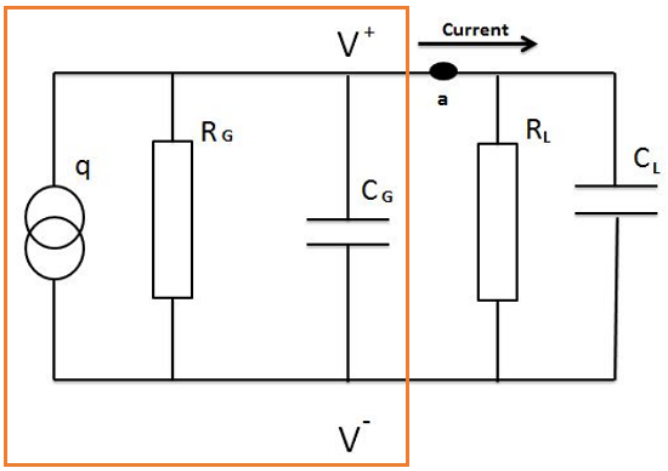

Fig.S5 Equivalent circuit model of a piezoelectric PVDF fiber-based power generator. The electrical circuit is parallel connected to an equivalent load resistor R_L and capacitor C_L. The electrospun generator can be equivalently modeled as a charge generator q and in parallel connection to a capacitor C_G and a resistor R_G. The positive output current is indicated in the figure.

The underlying mechanism for the energy generation in the drawn PVDF NMFs can be detailed in the following: as the strain is released from the power generator (PG), corresponding negative peaks can be observed in both the output voltage and current measurements. This phenomenon can be explained by examining the equivalent circuit model of the power generator in Fig.S5, as the reference cited in manuscript [44]

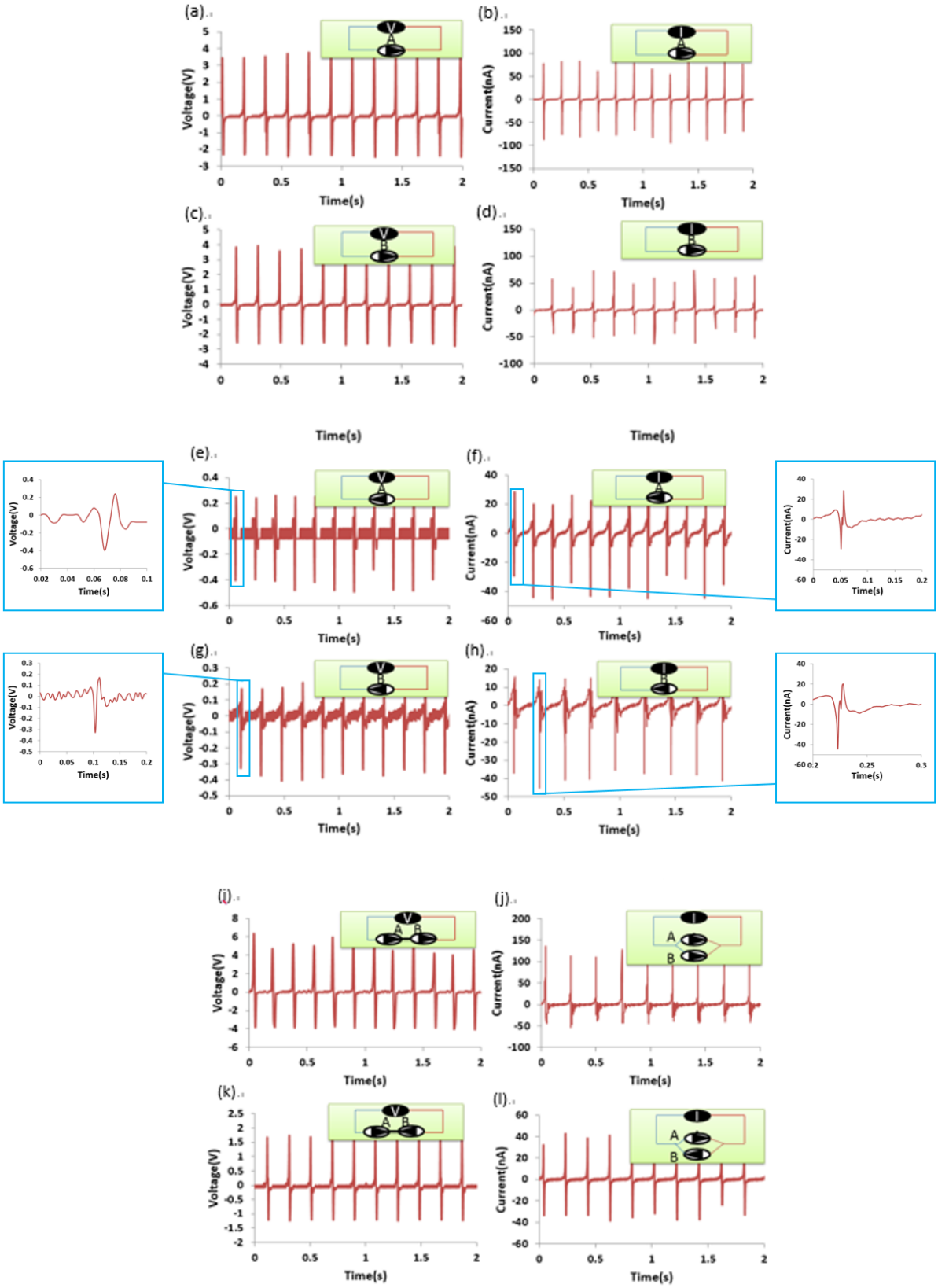
(a)
(b)
(c)
(d)
(e)
(f)
(g)
(h)
(i)
(j)
(k)
(l)
Voltage(V)
Current(nA)
Time(s)
V
I
A
B

Fig.S6 In the forward connection, Open-circuit voltage output and short-circuit current power output from PG A is shown in (a) and (b), respectively. In a similar fashion under forward connection (c) Open-circuit voltage output and (d)short-circuit current power output from PG B, respectively. In the reversal connection, Open-circuit voltage output and short-circuit current power output from PG A is shown in (e) and (f), respectively. In a similar fashion under reversal connection (g) Open-circuit voltage output and (h) short-circuit current power output from PG B, respectively. Serial connection of PG A and PG B demonstrates the effect of (i) voltage add up or (k) cancel out. Short-circuit current power output in both parallel connection of PG A and PG B also demonstrates that the PG is going through (j) add up or (l) cancel out. The connection configurations of the two PGs are specified in reference to the measurement system as indicated in all insets in above figures.

The detail of characterization for the true signals actually coming from output voltage and current of integrated PGs, are systematically presented in Fig.S6. Furthermore, the switching-polarity tests are also conformed for the two PGs, fully in agreement with published data and indicate the true signals are obtained from the fabricated PGs.

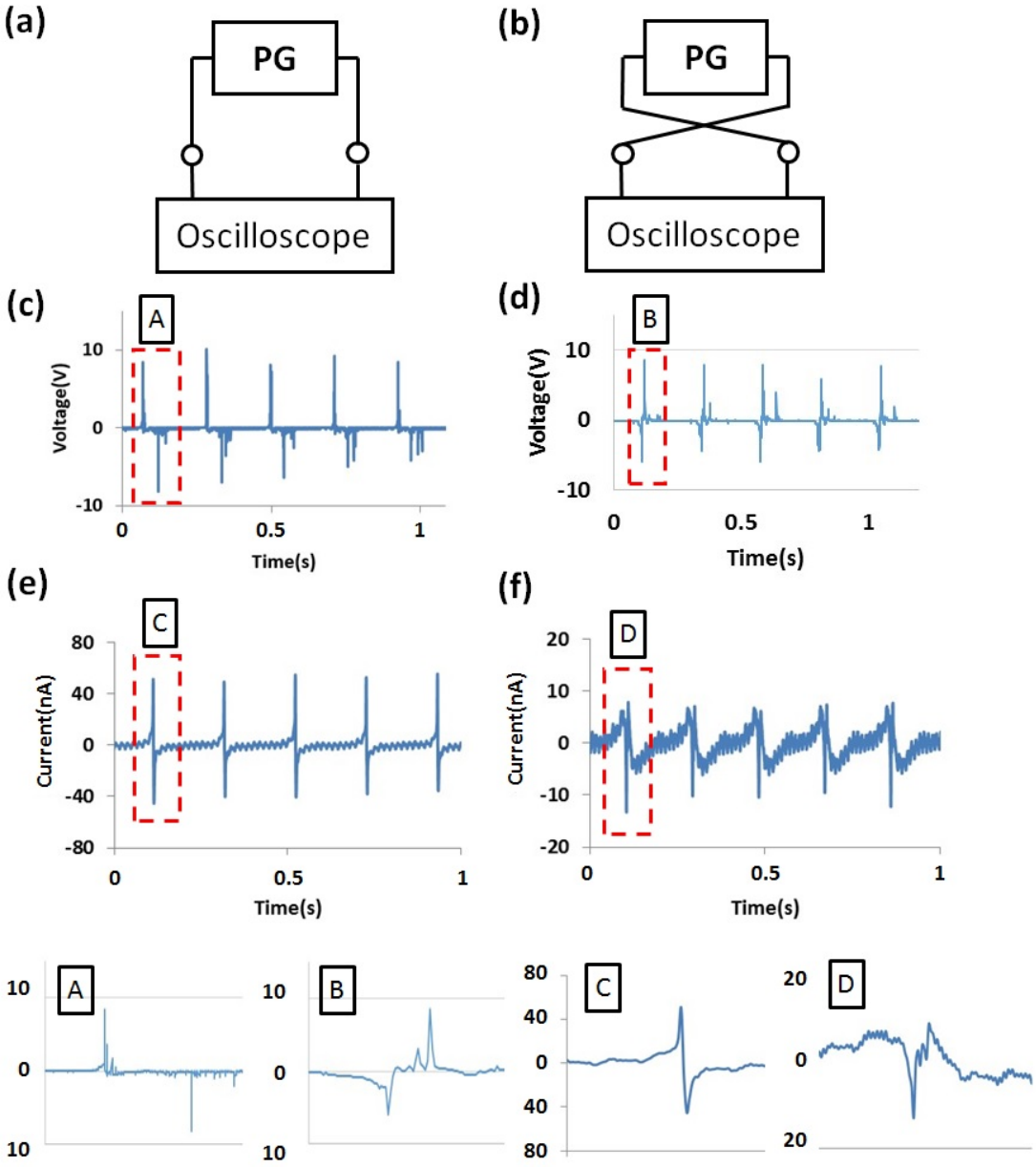

Fig.S7 Schematic illustration of polarity test under (a) forward and (b) reverse connections as well as related output voltage and current in (c)-(d) and (e)-(f), respectively. The experimental setup is made of a substrate with near-field electrospinning (NFES) deposited nano/micro fibers (NMFs) arrays that respond to the rotary motor actuation, while the operating frequency can be easily realized via the adjustment of rotary speed, as seen in the manuscript Fig. 2a. The substrate is rectangular polyvinyl chloride (PVC). As mechanical deformation was induced on the substrate, tensile strain and a corresponding piezoelectric potential in the NMFs can be created. The magnified pattern of one single bending and release process is illustrated in the bottom plots A-D. Peak voltage was measured to be about 10V in the

forward connection and 8V in the reverse connection, the peak current was measured to be 40nA in the forward connection and 8nA in the reverse connection, respectively. The flip of polarity can be clearly identified and validate the signals are from authentically piezoelectric output, at a frequency of 5 Hz and strain 0.5%

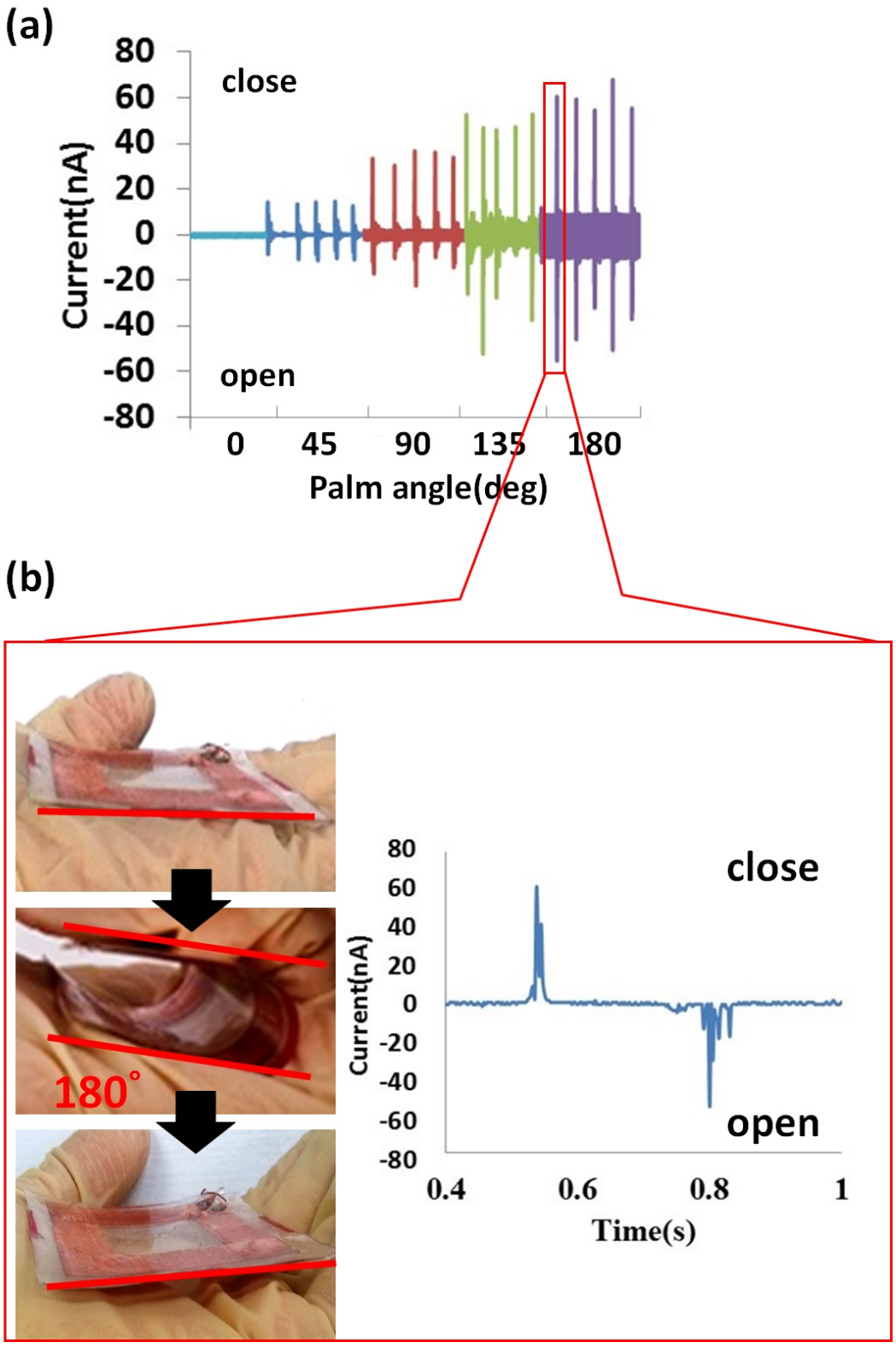

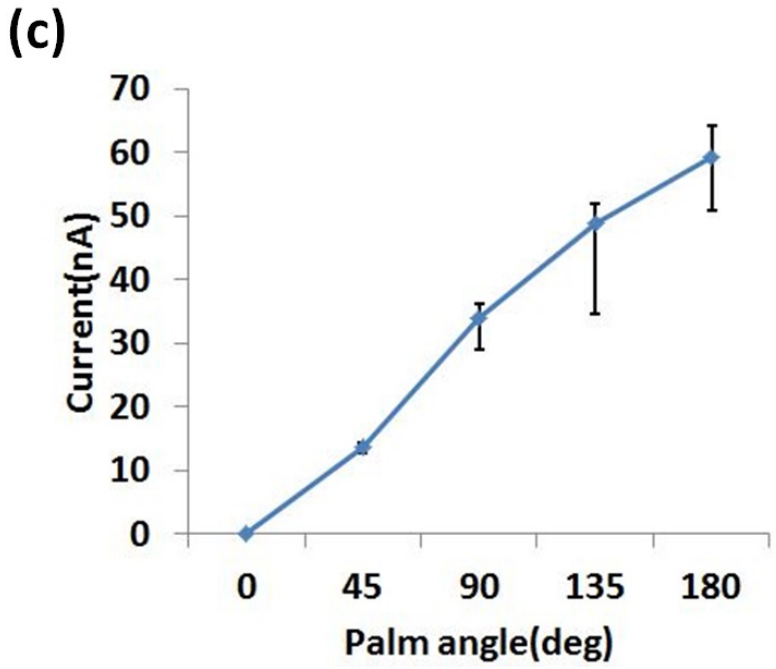

Fig.S8 Human palm-enabled PG using direct-write, in-situ poled NMFs and corresponding electrical measurements. The NMFs are initially NFES electrospun and deposited on the substrate with a predefined electrode pattern, completely encapsulated with Polydimethylsiloxane (PDMS) and attached on the palm. Experimentally, a cyclic compressive/tensile stress is induced as the palm folds and releases at various angles during the measurements. (a) Multiple events of palm folding-releasing actions and corresponding current outputs of a NMFs device at a frequency of approximately 2Hz. (b) A current output appeared on the event of the folding and releasing action of the palm held at a 2Hz cyclic motion and angle of ~ 180 °. (c) Effect of palm bends angle and electrical output. Measured current versus angle of palm bend angle. Error bars: standard deviation.

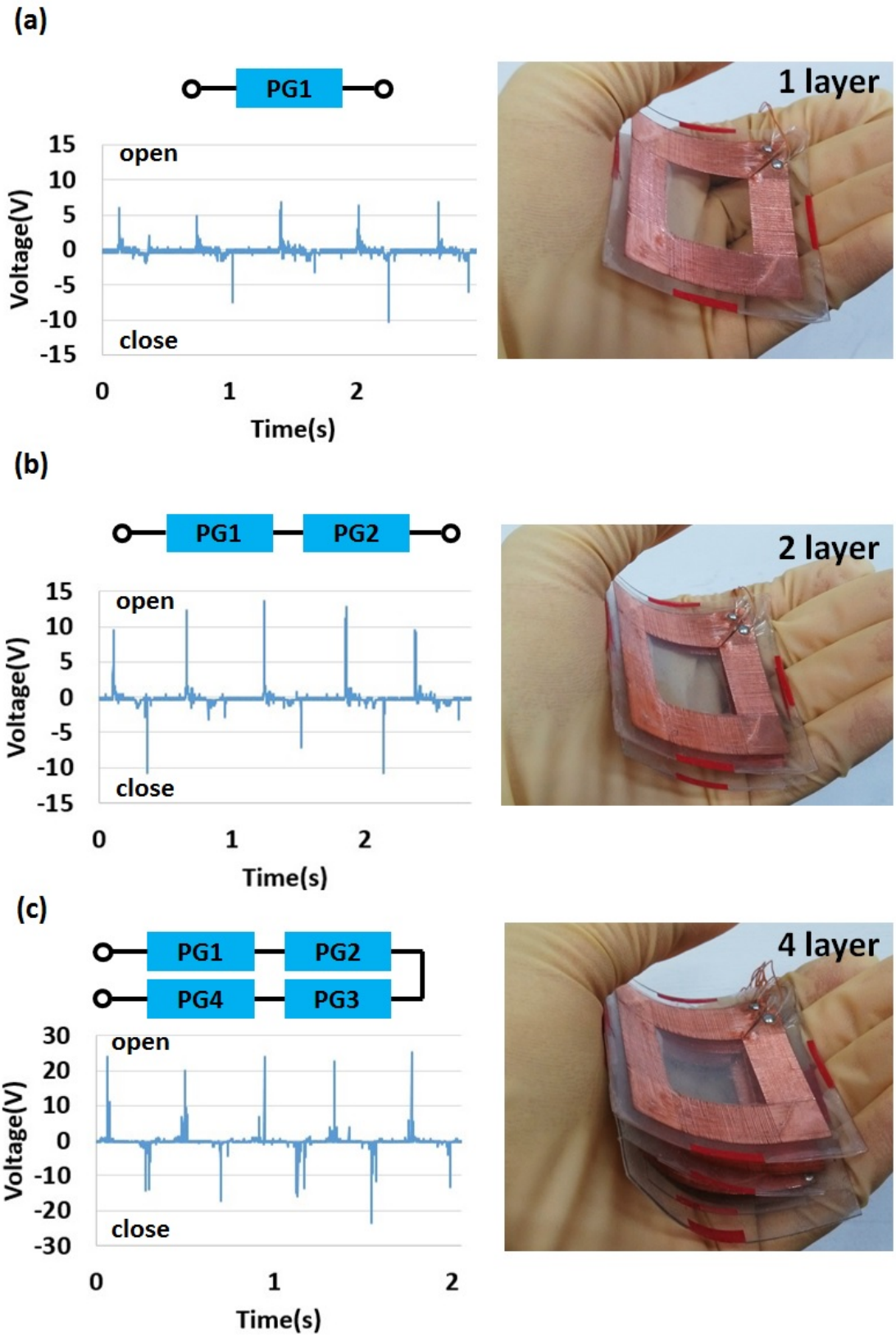

Fig.S9 A largely enhanced electrical output PG device integrated in series for voltage. Demonstration of the integrated PG to the feasibility of scale-up for enhancing the output voltage. The number of integrated layers in the series configurations is

experimentally demonstrated to have a direct impact on the output voltage. Output voltage of PGs integrated in series configuration, respectively with (a) one layer, (b) two layers, and (c) four layers, at a frequency of 3Hz. The basic principle of electrical voltage and current superposition in the serial/parallel configuration can be easily achieved and experimentally validated due to the direct-write nature of NFES technology.

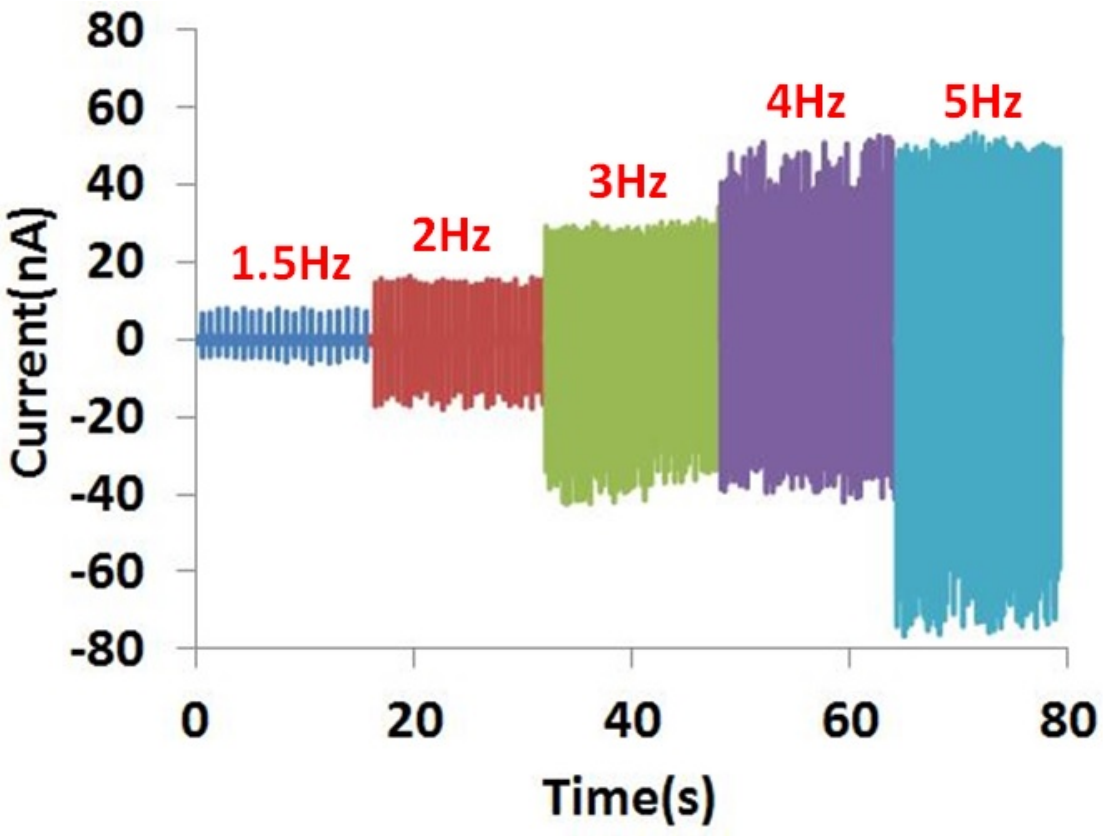

Fig.S10 The responses of the PG under various cycling frequencies ranging from 1.5 to 5 Hz for the same applied external strain of 0.5%. In the experimental setup, the cycling frequency can be directly related to the strain rate since the linear motor controls the stretch-release cycle for a given applied strain. Measurement results show that the output current increase proportionally to the increase of the cycling frequency during both the stretch and release cycles.

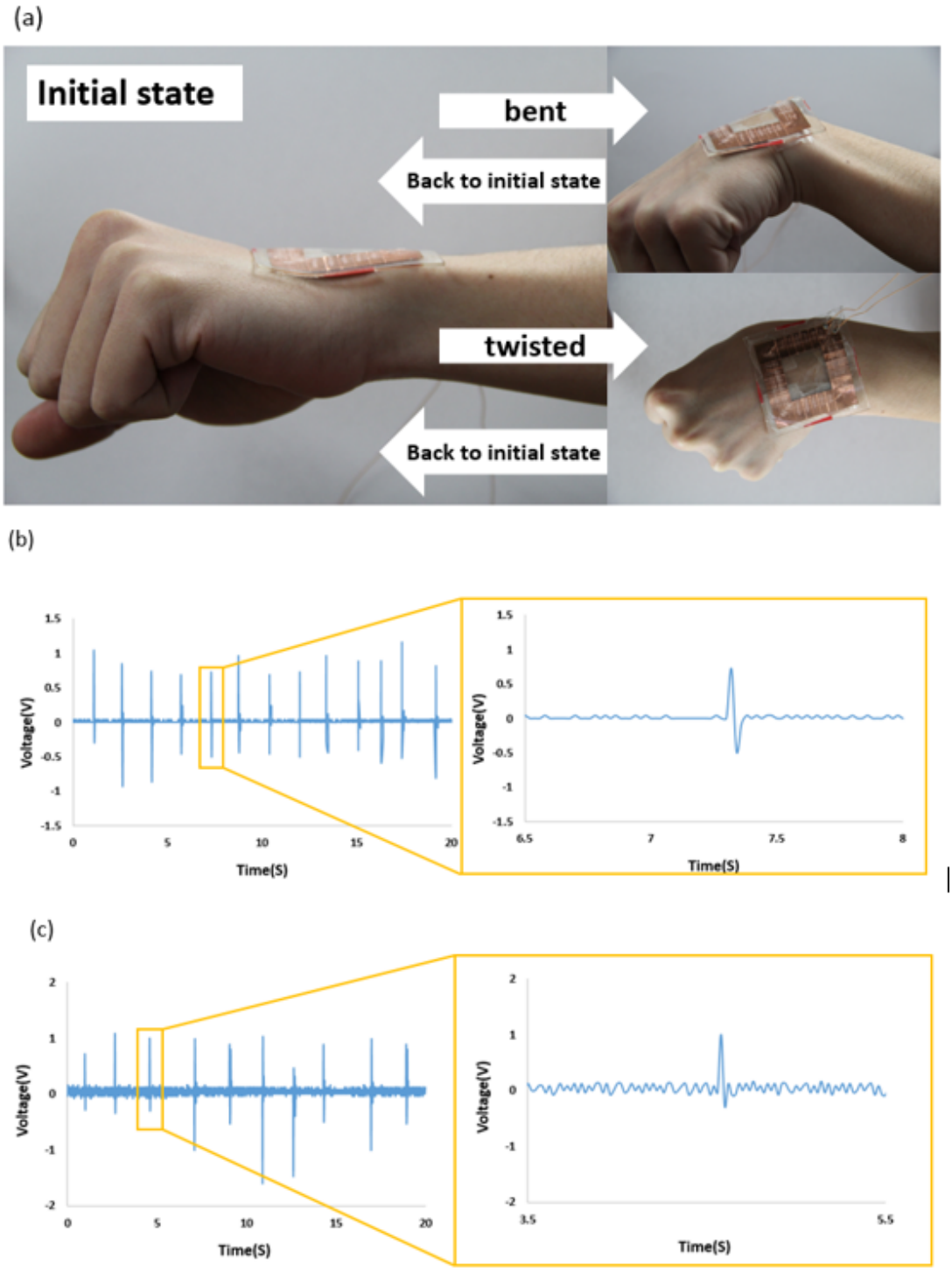

Fig.S11 Difference in terms of performance of the highly flexible PG as an active sensor operated by the left palm. Photographic image of the PG attached to the wrist joint such that two motions of bending and twisting are demonstrated in (a) Initial state, bent, and unbent to the initial state. Initial state, twisted, and unbent to the initial state in left. (b) Output voltage of the PG driven by bent left wrist. (c) Output voltage of the PG driven by torsion left wrist.